

## PHOTOELECTRIC EMISSION MEASUREMENTS ON THE ANALOGS OF INDIVIDUAL COSMIC DUST GRAINS

M. M. ABBAS,<sup>1</sup> D. TANKOSIC,<sup>2</sup> P. D. CRAVEN,<sup>1</sup> J. F. SPANN,<sup>1</sup> A. LECLAIR,<sup>2</sup> E. A. WEST,<sup>1</sup> J. C. WEINGARTNER,<sup>3</sup>  
A. G. G. M. TIELENS,<sup>4</sup> J. A. NUTH,<sup>5</sup> R. P. CAMATA,<sup>6</sup> AND P. A. GERAKINES<sup>6</sup>

Received 2005 July 13; accepted 2006 March 10

### ABSTRACT

The photoelectric emission process is considered to be the dominant mechanism for charging of cosmic dust grains in many astrophysical environments. The grain charge and equilibrium potentials play an important role in the dynamical and physical processes that include heating of the neutral gas in the interstellar medium, coagulation processes in the dust clouds, and levitation and dynamical processes in the interplanetary medium and planetary surfaces and rings. An accurate evaluation of photoelectric emission processes requires knowledge of the photoelectric yields of individual dust grains of astrophysical composition as opposed to the values obtained from measurements on flat surfaces of bulk materials, as it is generally assumed on theoretical considerations that the yields for the small grains are much different from the bulk values. We present laboratory measurements of the photoelectric yields of individual dust grains of silica, olivine, and graphite of  $\sim 0.09\text{--}5\ \mu\text{m}$  radii levitated in an electrodynamic balance and illuminated with UV radiation at 120–160 nm wavelengths. The measured yields are found to be substantially higher than the bulk values given in the literature and indicate a size dependence with larger particles having order-of-magnitude higher values than for submicron-size grains.

*Subject heading:* dust, extinction

*Online material:* color figures

### 1. INTRODUCTION

It is well recognized that submicron/micron-size cosmic dust grains play an important role in the evolution and dynamical processes in the galaxy, the interstellar medium (ISM), and the interplanetary and planetary environments. The dust grains in various astrophysical environments are generally charged, and their equilibrium charge and surface potential influence the dynamical and physical evolutionary processes (e.g., Bailey & Williams 1988; Harwit 1998; Field & Cameron 1975; Draine 2004). The dust grains in space environments may be charged by a variety of mechanisms that include collisional processes with electrons and ions, triboelectric charging, and photoelectric emissions (e.g., Wyatt 1969; Feuerbacher et al. 1973; Draine 1978; Draine & Sutin 1987).

The photoelectric emission process is believed to be the dominant process in many astrophysical environments with nearby ultraviolet (UV) sources, such as the ISM, diffuse clouds, outer regions of the dense molecular clouds, interplanetary medium, dust in planetary environments and rings, cometary tails, etc. The photoelectric emission from dust grains is assumed to be an important mechanism for heating of the neutral gas in the diffuse interstellar clouds, as well as in the surface regions of the molecular clouds, and is believed to play an important role in the dynamical evolution of the ISM (e.g., Watson 1972, 1973; Draine

1978; Mukai 1981; Bakes & Tielens 1994; Dwek & Smith 1996; Weingartner & Draine 2001). The charge and equilibrium potentials of dust grains influence the coagulation and condensation processes in molecular clouds. The photoelectric emission process is also the dominant dust-charging process on the lunar sunlit environment leading to levitation and transportation of dust on the lunar surface observed during the *Apollo* missions (e.g., Feuerbacher et al. 1972; Pelizzari & Criswell 1978; Horanyi et al. 1995, 1998, 1998b; Stubbs et al. 2006).

An evaluation of the charge and equilibrium surface potential of dust grains of various astrophysical compositions induced by photoelectric emissions requires knowledge of the photoelectric yield defined as the electrons emitted per photon absorbed. Accurate theoretical models for calculation of the yields of individual dust grains are not yet available, and the required information has to be obtained by laboratory measurements. However, the only measurements of photoelectric yields available in the literature for dust materials of astrophysical composition are those made on bulk materials with flat surfaces. This situation exists even though it has long been postulated on theoretical considerations that the photoelectric yields of individual dust grains would be substantially different from those for the corresponding bulk materials (e.g., Watson 1972, 1973; Gallo & Lama 1976a, 1976b; Draine 1978). The photoelectric yields of small nanometer-size gold and silver particles suspended in He gas and irradiated by UV were measured in a series of papers (Schmidt-Ott et al. 1980; Burtcher & Schmidt-Ott 1982; Burtcher et al. 1984). The measurements apparently indicated strong enhancements in the yields compared with the bulk values for Ag particles, but no enhancement for the Au particles. However, the latter paper (Burtcher et al. 1984) showed that for clean Ag particles, the yield curve was similar to that for the bulk values, indicating that the measured enhancement was affected by the surface contaminants. The existing models have not provided a satisfactory explanation for the observed data.

<sup>1</sup> NASA Marshall Space Flight Center, Huntsville, AL 35812; mian.m.abbas@nasa.gov, paul.d.craven@nasa.gov, james.f.spann@nasa.gov, edward.a.west@nasa.gov.

<sup>2</sup> University of Alabama, Huntsville, AL 35899; tankosd@uah.edu, andre.leclair@msfc.nasa.gov.

<sup>3</sup> George Mason University, Fairfax, VA 22030; joe@physics.gmu.edu.

<sup>4</sup> Kapteyn Astronomical Institute, Groningen, Netherlands; tielens@astro.rug.nl.

<sup>5</sup> NASA Goddard Space Flight Center, Greenbelt, MD 20771; joseph.a.nuth@nasa.gov.

<sup>6</sup> Department of Physics, University of Alabama, Birmingham, AL 35294; camata@uab.edu, gerakines@uab.edu.

Several theoretical models based on classical electrostatics have been proposed that indicate an inverse size dependence of  $\sim 1/a$  for ionization threshold energy or the work function (WF). A considerable amount of data now exists for experimental determination of the ionization threshold energy of particles extending in size over the range of clusters of a few atoms, nanometer/micron-size particles, and progressively merging with the bulk materials (e.g., Gallo & Lama 1974, 1976a, 1976b; Ekardt 1985; Seidl et al. 1991; Bréchnignac et al. 1992; Dugourd et al. 1992; de Heer 1993; Wong et al. 2003). No direct photoelectric yield measurements on individual dust grains of astrophysical interest have been reported as yet.

In this paper, we present the first measurements of the photoelectric yields of individual submicron/micron-size dust grains of astrophysical interest. The yields reported here were determined by direct measurements of the discharge rates of negatively charged dust grains of silica, olivine, and carbonaceous composition, with sizes in the range of 0.09–5  $\mu\text{m}$  radii. The measurements were made by levitating individual grains of known size and composition in an electrodynamic balance and illuminating them with UV radiation of known intensity at wavelengths of 120, 140, and 160 nm. In § 2, a description of the experimental apparatus employed in the measurement is given with a brief review of the electrodynamic balance. The basic equations and the methodology employed for photoelectric emission and yield calculations are given in § 3. Experimental results of the photoelectric efficiencies and yields of silica, olivine, and carbonaceous dust grains are given in § 4, with a detailed discussion of the possible sources of errors in the measurements in § 5. In § 6, we discuss some theoretical considerations relevant to photoelectric emissions. A summary and conclusions of the measurements are given in § 7.

## 2. EXPERIMENTAL APPARATUS

### 2.1. Electrodynamic Balance

The photoelectric emission measurements reported here were performed on an electrodynamic balance, also referred to as a quadrupole trap, that permits levitation of a single micron-size dust grain in simulated astrophysical environments. An electrodynamic balance consists of a top and a bottom electrode of hemispherical configuration, and a ring electrode of cylindrical configuration. The top and bottom electrodes are kept at positive or negative DC potentials ( $V_{\text{DC}}$ ) with respect to the ground, depending on the polarity of the dust grain charge, and an AC potential ( $V_{\text{AC}}$ ) is applied to the cylindrical electrode. The net effect of the AC field is to produce a null potential at the geometric center of the cavity with the DC electric field balancing the gravitational force on a charged dust grain. The dust grains may be kept trapped in the balance for extended periods as long as the required AC and DC potentials and the AC frequency ( $\Omega = 2\pi f$ ) satisfy the stability conditions for keeping the particle at the balance center. The stability conditions are determined by the field and drag factors  $\beta$  and  $\xi$ , respectively, defined as

$$\beta = \frac{2g}{C_0 z_0 \Omega^2} \frac{V_{\text{AC}}}{V_{\text{DC}}}, \quad (1)$$

$$\xi = \frac{18\eta}{\rho \Omega D^2}, \quad (2)$$

where  $\eta$  is the viscosity of air,  $\rho$  is the mass density of the particle,  $g$  is the gravitational acceleration,  $C_0$  is a geometric constant experimentally determined to be 0.68,  $z_0 = 0.750$  cm is

the distance from the trap center to the DC electrodes, and  $D$  is the effective particle diameter. A particle is trapped only under a certain range of values of  $\beta$  and  $\xi$  as determined by stable solutions of the equations of motion of the particle. A detailed description of the principles, basic equations, and the required apparatus has been given in previous publications (e.g., Davis 1985; Spann et al. 2001; Abbas et al. 2002a, 2002b, 2003, 2004).

A basic quantity that is experimentally determined on the electrodynamic balance with a particle stably trapped is the charge-to-mass ratio given by

$$\frac{q}{m} = \frac{gz_0}{C_0 V_{\text{DC}}}. \quad (3)$$

With direct measurements of  $V_{\text{DC}}$ , the charge-to-mass ratio of a trapped particle given by equation (3) is a directly measurable quantity and forms the basis of all measurements on an electrodynamic balance.

### 2.2. Experimental Setup and Procedure for Photoelectric Emission Measurements

The experimental setup for photoelectric emission measurements is shown in a schematic in Figure 1 and consists of the following main components:

1. *Electrodynamic balance*: Top and bottom hemispherical electrodes, and a cylindrical ring electrode in a vacuum chamber with suitable viewing ports.

2. *Electric power supplies*: Consisting of an AC voltage source ( $V_{\text{AC}} \sim 100\text{--}2000$  V, at  $f_{\text{AC}} \sim 10\text{--}1000$  Hz), a low DC voltage source ( $V_{\text{DC}} \sim 0.01\text{--}50$  V), and a DC high-voltage source ( $V_h \sim 0\text{--}1000$  V) power supply for inductive charging of the dust particles.

3. *Particle injector*: A pressure impulse device to inject an inductively charged particle (positive or negative) of known composition and density in the balance through a port at the top (Spann et al. 2001).

4. *Particle imaging system*: A 15 mW, He-Ne laser with an optical magnifying system to project the image of the levitated particle on a monitor.

5. *Vacuum system*: With leak valves and pressure gauges for controlled evacuation of the chamber pressures to  $\sim 10^{-4}$  to  $10^{-5}$  torr.

6. *Far-UV source*: A *deuterium lamp* with  $\text{MgF}_2$  window, focusing equipment, and a vacuum monochromator with FWHM resolution of 8 nm. The UV beam is collimated and focused with a  $\text{MgF}_2$  lens to limit the beam diameter  $\sim 3.5\text{--}4.5$  mm (FWHM) size, smaller than the 6 mm entry/exit apertures in the balance ring electrodes, thus eliminating or minimizing photoelectrons emitted by the walls due to any stray UV radiation.

7. *Photomultiplier tube (PMT)*: With spectral response in the 115–200 nm wavelength region.

The size or the “effective” diameter of a trapped particle is determined from a few “spring-point” measurements at pressures of  $\sim 1\text{--}10$  torr. The size calculations are based on marginal instability of the levitated particle involving the field and viscous drag factors defined in equations (1) and (2), and are discussed in more detail in § 5.1 and in previous publications (e.g., Davis 1985; Spann et al. 2001). Estimates or upper limits of the particle sizes may also be obtained from the monitor images using scale factors developed from particles of known sizes  $\geq 5$   $\mu\text{m}$ . After stable trapping and size determinations at pressures of  $\sim 1\text{--}10$  torr, a controlled evacuation procedure is started to allow

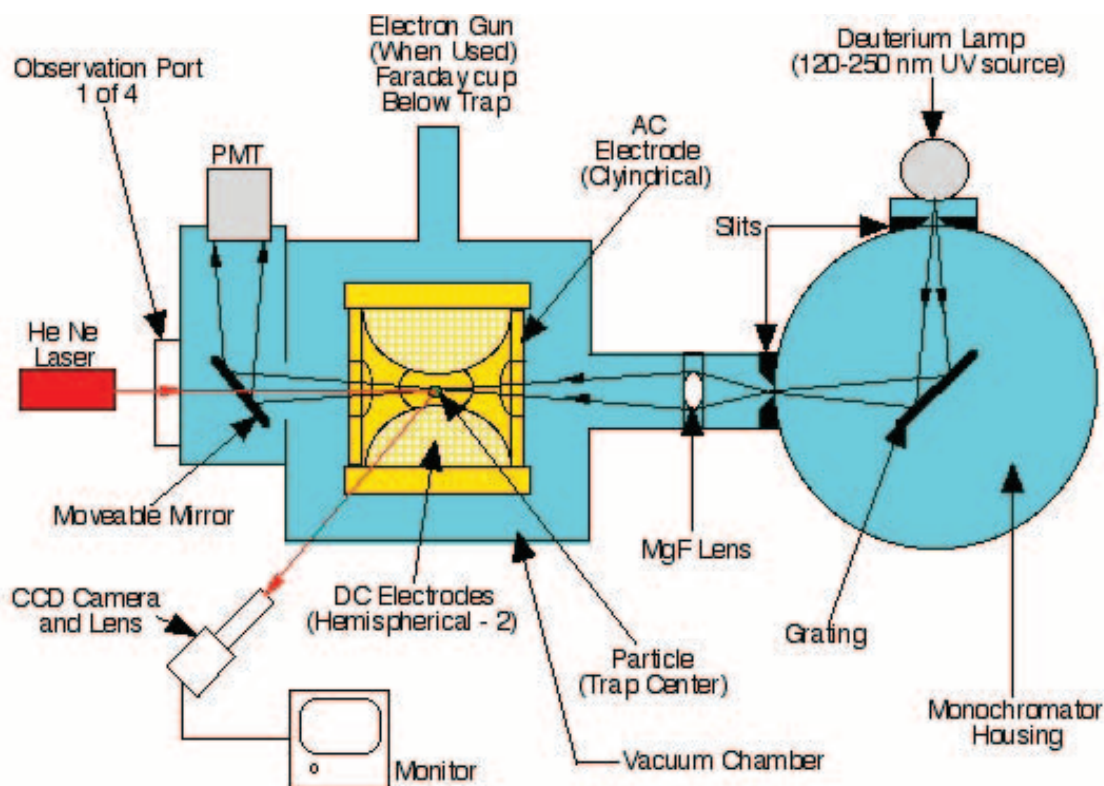


Fig. 1.—Schematic of the setup of an electrodynamic balance for UV photoelectric yield measurements.

the chamber pressure to reach  $\sim 10^{-4}$  to  $10^{-5}$  torr, at which the photoelectric emission measurements on the levitated particles are carried out.

The levitated particles in the trap are charged positively or negatively by an inductive process with a high DC potential in the particle injector, the sign of the charge being selected by the polarity of the charging voltage. A negatively charged particle may be discharged by exposing it to UV radiation, and a positively charged one discharges through exposure to a low-energy electron beam. The initial magnitude of charge on a grain is controlled to a degree by the DC potential employed for the charging process. A typical charge for measurements on silica grains, for example, varied from  $\sim 30$ – $100$  electrons for particles of  $\sim 0.1 \mu\text{m}$  radii to  $>200,000$  electrons for particles of  $>3$ – $5 \mu\text{m}$  radii. When the UV radiation beam is turned on, the particle begins to discharge by ejecting electrons at a rate that depends on the radiation intensity, the size, and the charge state of the particle. The DC voltage is continuously adjusted to balance the gravitational force and keep the particle at the trap center. The UV radiation may be turned on or off, with the particle discharging or maintaining a constant charge, respectively. The particle is ejected from the balance when it is nearly or completely discharged.

A positively charged polystyrene particle of  $2.3 \mu\text{m}$  radius was kept trapped in the electrodynamic balance for a period of about 8 days for test purposes and was periodically discharged and charged by exposure to an electron beam of  $50$ – $2500 \text{ eV}$  and a UV radiation beam, respectively. A cycle of discharging and charging of the trapped particle selected from a portion of the data obtained over a period of about 5.5 hr is shown in Figure 2. With UV radiation at  $160 \text{ nm}$  wavelength turned on at  $t \sim 1060$  minutes, the particle charge increases from an initial charge  $q \sim 840e$  to  $\sim 880e$  at  $t \sim 1170$  minutes. At this time, the UV

radiation intensity is changed to a much stronger value consisting of “white light” covering all wavelengths in the visible to  $120 \text{ nm}$  spectral region, and the particle charge rapidly increases to an equilibrium value of  $q \sim 1280e$  at  $t \sim 1270$  minutes. At  $t \sim 1360$  minutes the particle is now exposed to an electron beam at  $2500 \text{ eV}$ , and the particle discharges to  $q \sim 880e$  at  $t \sim 1380$  minutes. At this time the electron beam is turned off, the white light with UV radiation is turned on, and the particle charge increases again to the equilibrium value of  $\sim 1280e$  at  $t \sim 1500$  minutes. It should be noted that the scatter in the grain

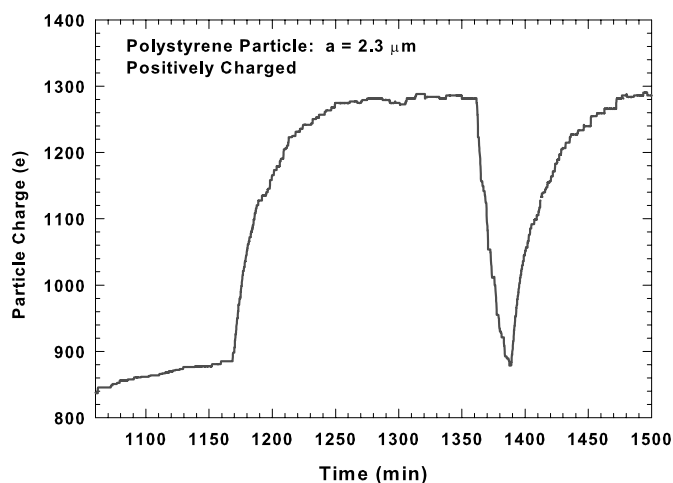


Fig. 2.—Variation of charge with time of a positively charged polystyrene particle of  $2.3 \mu\text{m}$  radius periodically discharged with an electron beam and charged with a UV photon beam. [See the electronic edition of the *Journal* for a color version of this figure.]

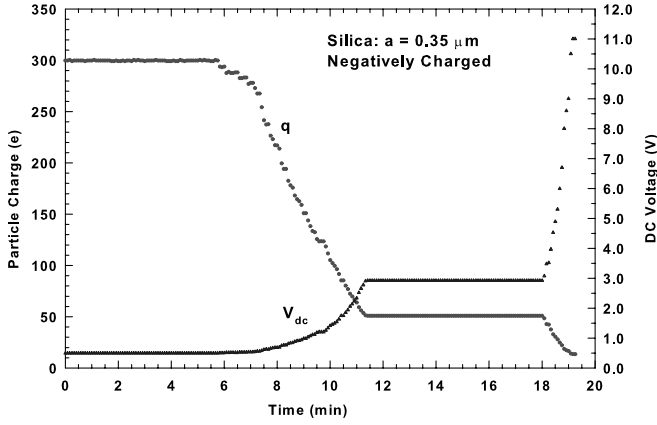


FIG. 3.—Variation with time of the charge and DC voltage of a  $0.35 \mu\text{m}$  radius silica particle, with the UV radiation beam turned on at  $t \sim 5$  minutes, off at  $\sim 11$  minutes, and on again at  $\sim 18$  minutes. The charge remains constant with the UV radiation off and discharges when it is turned on. The particle is ejected from the trap when the charge approaches zero. [See the electronic edition of the *Journal* for a color version of this figure.]

charge seen in Figure 2 reflects only the random variability of the DC voltage  $V_{\text{DC}}$ , the measurement accuracy of which is limited to  $\sim 1$  mV.

An example of the discharging of a  $0.35 \mu\text{m}$  radius silica particle with an initial negative charge of  $\sim -300e$  is shown in Figure 3. The particle maintains constant charge for about 5 minutes until it is exposed to UV radiation at  $160 \text{ nm}$  wavelength when it discharges to about  $50e$  in  $\sim 6$  minutes. With the UV radiation turned off, the charge remains constant until the UV is turned on again at  $t \sim 18$  minutes when the particle discharges to  $< 10e$  when it is ejected from the trap.

All photoelectric emission measurements reported in this paper were made on negatively charged dust grains. The choice of negative charge was made in view of the ease with which negatively charged particles may be discharged over a range of potentials from high to negligibly small values. Measurements on positively charged grains over a desired range of potentials may be made with a sequence of charging and discharging processes with UV and an electron beam, respectively, and are planned in the future.

### 3. CALCULATION OF PHOTOELECTRIC YIELDS

The photoelectric yield calculations are based on measurements of the discharge rate of a particle irradiated with a UV beam of known photon flux density. The photon flux in the beam is determined by reflecting it to a PMT and measuring the collected current, with the beam width determined by direct measurements at the trap center, as well as by modeling calculations using the ZEMAX optical software. With the beam width smaller than the projected area of the PMT, the number of photons per second in the beam  $N_B^{\text{ph}}$  and incident on the PMT is given by

$$N_B^{\text{ph}} = \frac{i_{\text{PMT}}(\lambda)}{e\eta_q(\lambda)GR}, \quad (4)$$

where  $i_{\text{PMT}}(\lambda)$  is the current measured by the PMT at wavelength  $\lambda$ ,  $e$  is the electron charge,  $\eta_q$  is the quantum efficiency,  $G$  is the gain of the PMT, and  $R$  represents the reflectance of the mirror (Fig. 1). To determine the number of photons per second incident on a dust grain levitated at the trap center, we as-

sume the radial distribution of photons in the beam to be of the Gaussian form as

$$n_B^{\text{ph}} = n_{\text{max}}^{\text{ph}}(0) \exp\left(-\frac{r^2}{r_e^2}\right), \quad (5)$$

where  $r_e = w_e/2$  represents the half-width of the beam where the photon flux density  $n_B^{\text{ph}}$  is  $1/e$  of the maximum value  $n_{\text{max}}^{\text{ph}}(0)$  at the beam center. The above assumption implies that the total integrated photon flux in the beam and measured by the PMT is represented by

$$N_B^{\text{ph}} = (\pi r_e^2) n_{\text{max}}^{\text{ph}}(0). \quad (6)$$

Since the beam width  $w_e \sim 3.5\text{--}4.5 \text{ mm}$  is much larger than the particle diameters, equations (4) and (6) may be used to calculate the number of photons incident on the dust grain per second with

$$n_d^{\text{ph}} = \frac{i_{\text{PMT}}(\lambda)}{e\eta_q(\lambda)GR} \frac{D_{\mu\text{m}}^2}{w_e^2(\lambda)}. \quad (7)$$

Using numerical values of the PMT used in the photoelectric emission experiments discussed in this paper, with the gain  $G = 600$  and  $R = 0.6$ , equation (7) may be written as

$$n_d^{\text{ph}} = 1.73 \times 10^{16} \frac{i_{\text{PMT}}(\lambda)}{\eta_q(\lambda)} \frac{D_{\mu\text{m}}^2}{w_e^2(\lambda)}. \quad (8)$$

To calculate photoelectric efficiencies and yields, the number of electrons emitted by a grain with the incident UV photons needs to be determined. This information may be obtained from the grain charge  $q(t)$  measured as a function of time (eq. [3]) and can be written in terms of the current  $i_d$  to the grain as

$$n_d^e(\phi_s) = \frac{i_d}{e} = \frac{1}{e} \frac{\partial q}{\partial t}. \quad (9)$$

The photoelectric efficiency of the dust grain is defined as the number of electrons emitted by the dust grain per incident photon, is a function of the surface potential  $\phi_s$ , and is written as

$$E_{\text{pe}} = \frac{n_d^e(\phi_s)}{n_d^{\text{ph}}}. \quad (10)$$

The photoelectric yield, however, is generally defined in the literature as photoelectrons emitted per photons absorbed with the grain potential approaching zero and may be written as

$$Y = \frac{E_{\text{pe}}}{Q_{\text{abs}}} = \frac{n_d^e(\phi_s \rightarrow 0)}{n_d^{\text{ph}} Q_{\text{abs}}}, \quad (11)$$

where  $Q_{\text{abs}}$  is the absorption efficiency of the grain and may be obtained by using Mie scattering theory calculations, assuming spherical particles with effective diameters  $D$  and a complex refractive index corresponding to the grain material. The use of effective diameters for nonspherical, irregularly shaped particles leads to an uncertainty in evaluation of  $Q_{\text{abs}}$  in the Mie theory calculations and is expected to produce scatter in the measured yield data representing the randomness of the particles. Equations (8)–(11) form the basis for measurement and calculation

of the photoelectric efficiency and yield of individual dust grains suspended in the trap and illuminated by UV radiation.

#### 4. EXPERIMENTAL RESULTS OF PHOTOELECTRIC YIELDS

Measurements of photoelectric efficiencies and yields have been carried out on micron/submicron-size grains of silica, olivine, and graphite levitated in the electrodynamic balance with the procedure outlined above. An emitted electron from the negatively charged grains employed in all experiments discussed in this paper experiences a repulsive Coulomb force that is a function of the grain charge or its surface potential. A repulsive force is exerted on an ejected electron in addition to a force due to image potential that is attractive regardless of the polarity of the dust grain charge. The photoelectric efficiency is thus expected to be higher for heavily charged negative grains at high surface potentials compared with the values when the grain is close to being completely discharged with the surface potential approaching zero. The photoelectric efficiency defined in equation (10) is a function of the particle surface potential, and the measurements generally show an upward trend with higher potentials. The photoelectric yield, however, is generally defined for neutral bulk materials with zero surface potential and is represented by the photoelectric efficiency with the surface potential approaching zero. To determine the photoelectric yield from the measurements, we adopt the procedure of least-squares regression to determine the efficiency for the potential approaching zero. This value of photoelectric efficiency when convolved with the absorption efficiency  $Q_{\text{abs}}$  represents the photoelectric yield in accordance with the definition of equation (11). The absorption efficiency is calculated by using the Mie scattering theory (e.g., Bohren & Huffman 1983; Wiscombe 1979) for the measured effective radius of the particle determined by the spring-point method. The photoelectric yields in the composite yield plots given in §§ 4.1–4.3 have been determined from the efficiency measurements with the procedure indicated above.

##### 4.1. Photoelectric Yields of Silica Grains

The silica grains employed in the measurements presented here were obtained from the Bangs Laboratories, Indiana, and have been used for radiation pressure measurements as reported in a previous publication (Abbas et al. 2003). These grains of spherical configuration, with known density and complex refractive index, are calibrated to the nominal sizes and are thus particularly suitable for investigating the effects of grain size on photoelectric emissions under UV irradiation. In particular, the experiments were performed on grains selected from five bins calibrated to sizes of 0.13, 0.35, 0.75, 1.5, and 3.4  $\mu\text{m}$  radii. The accuracy of the nominal particle sizes was verified by carrying out spring-point measurements with standard deviations of  $\sim 5\%$ – $6\%$  in the nominal radii. Photoelectric emission measurements were made on several negatively charged particles of each size selected from each bin, with UV radiation at 120, 140, and 160 nm wavelengths. The measurements are repeated in cycles at several different particle surface potentials ( $\phi_s$ ) as the particles discharge and the surface potentials change with time. The results presented here represent measurements on 21 silica particles of radii in the 0.13–3.4  $\mu\text{m}$  range. The averaged values of the photoelectric efficiencies calculated as a function of surface potentials generally indicate higher values at higher potentials. The plotted yields, however, represent the efficiency measurements at the grain charge  $Z$  or potential approaching zero as discussed above.

Figures 4a–4c represent plots of the average photoelectric efficiencies of silica particles of radii 0.35, 1.5, and 3.4  $\mu\text{m}$  at UV

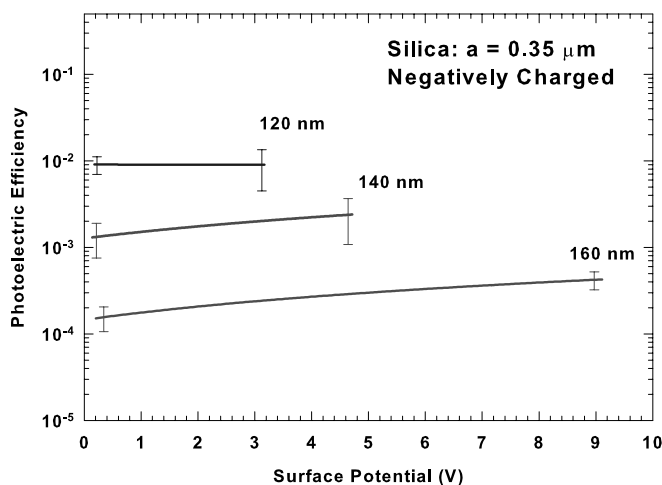


FIG. 4a

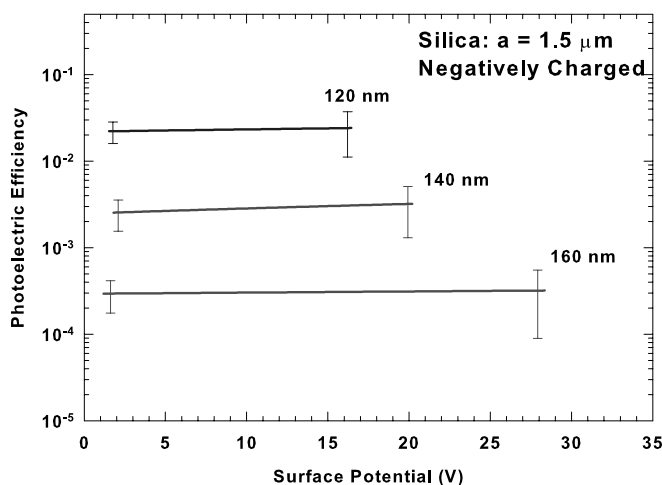


FIG. 4b

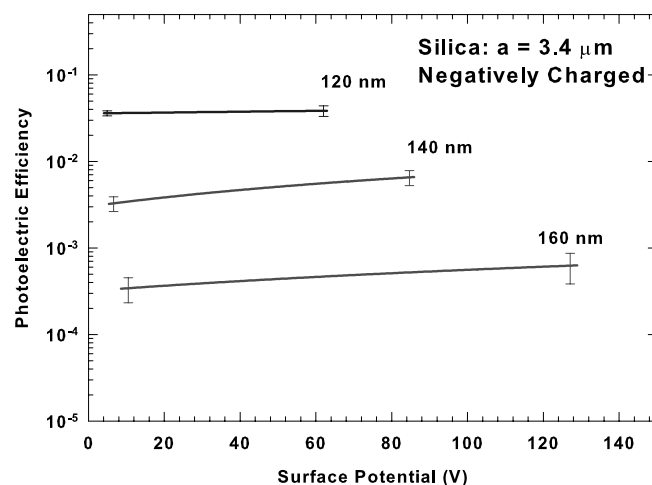


FIG. 4c

FIG. 4.—(a)–(c): Average photoelectric efficiencies as a function of the particle surface potential based on measurements on a number of silica particles of 0.35, 1.5, and 3.4  $\mu\text{m}$  radii illuminated with UV radiation at 120, 140, and 160 nm wavelength. The error bars indicate the  $1\sigma$  standard deviation due to the variability of the particles' size, as well as the measurement errors. [See the electronic edition of the *Journal* for a color version of this figure.]

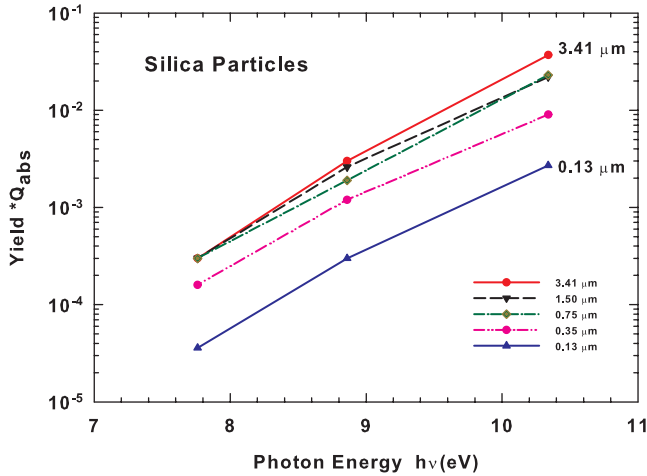


FIG. 5.—Photoelectric yields ( $*Q_{\text{abs}}$ ) vs. photon energy averaged over measurements on several silica particles.

wavelength of 120, 140, and 160 nm, corresponding to photon energies of 10.3, 8.9, and 7.9 eV, respectively. Each plot is based on measurements on four to five particles of the same nominal radius, and the error bars indicate the  $1\sigma$  variability in the measured data representing the measurement errors, as well as the variability in the particle size. Figure 5 represents the photoelectric yields ( $*Q_{\text{abs}}$ ) deduced from the photoelectric measurements on all silica particles and plotted as a function of the photon energy. The measurements indicate an exponential increase in the yields ( $*Q_{\text{abs}}$ ) with photon energy and a general trend of higher yields for larger size particles.

The photoelectric yield, defined as the number of electrons ejected per photons absorbed is determined by dividing the efficiencies corresponding to zero grain surface potentials by the absorption efficiency  $Q_{\text{abs}}$  of the particles, is plotted in Figure 6 as a function of the size parameter  $x = (2\pi a/\lambda)$ , where  $a$  is the grain radius and  $\lambda$  is the wavelength. This parameter is calculated by using Mie scattering theory (e.g., Bohren & Huffman 1983; Wiscombe 1979) with the complex refractive indices deduced from the data given by Draine & Lee (1984). Using the data shown in Figure 6, the photoelectric yields  $Y$  of all silica particles

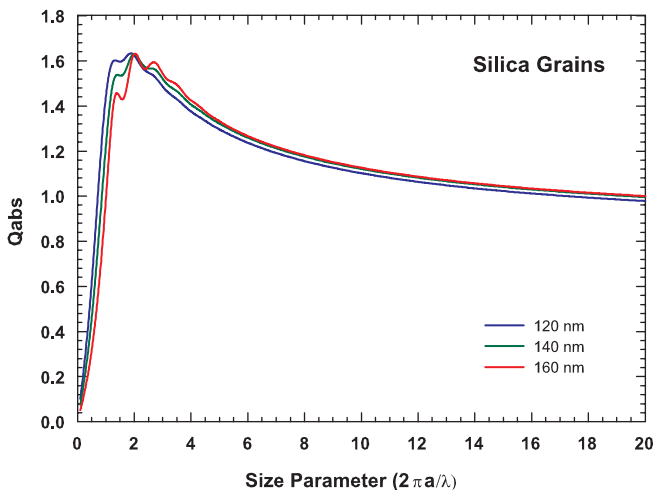


FIG. 6.—Absorption efficiency  $Q_{\text{abs}}$  of silica particles as a function of the size parameter ( $2\pi a/\lambda$ ), using Mie scattering theory, with complex refractive indices from the data in Draine & Lee (1984).

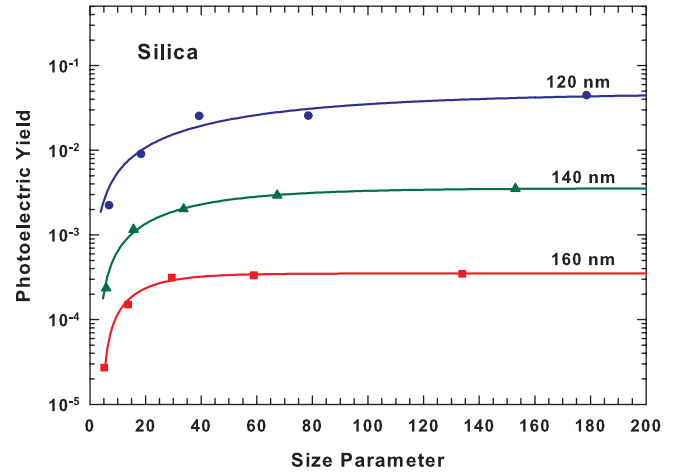


FIG. 7.—Photoelectric yields  $Y$  of all particles of 0.13, 0.35, 0.75, 1.5, and 3.4  $\mu\text{m}$  radii measured at UV wavelengths of 120, 140, and 160 nm (10.3, 8.9, and 7.9 eV, respectively) as a function of the size parameter  $x = (2\pi a/\lambda)$ .

are shown in Figure 7 as a function of the size parameter. Figure 7 indicates the photoelectric yields increasing with the particle size for all three wavelengths reaching asymptotic values for large particles. For large particles, the yields for all three wavelengths of 120, 140, and 160 nm, with photon energies of 10.3, 8.9, and 7.9 eV, respectively, are seen to approach asymptotic values that may be assumed to correspond to the bulk values.

#### 4.2. Photoelectric Yields of Carbonaceous Grains

The carbonaceous grains employed in the measurements were synthesized in a laboratory at the University of Alabama at Birmingham and are of nonspherical and irregular configuration with sizes in the range of  $\sim 0.1$ – $5\ \mu\text{m}$  radii. The particle sizes were determined by the spring-point measurements as discussed in § 3.2, and the density was estimated to be  $\sim 2.0\ \text{g cm}^{-3}$ , consistent with the irregular shape and porous nature of the particles. Typical examples of the photoelectric efficiency measurements as a function of the particle surface potentials are shown in Figures 8a and 8b for two particles of 0.44 and 4.5  $\mu\text{m}$  radii. A composite plot of the photoelectric yield measurements on all carbonaceous particles is shown in Figure 9 as a function of the size parameter. Also shown for comparison are the measurements by Feuerbacher & Fitton (1972) made on a bulk carbonaceous material for three photon energies of 10.3, 8.9, and 7.8 eV (120, 140, and 160 nm, respectively). The plotted bulk measurements have been corrected by using the reflectivities indicated by Feuerbacher & Fitton (1972) to correspond with the yields presented here as electrons emitted per photon absorbed. The measurements shown for the individual dust grains are seen to be higher than the corresponding bulk values by factors of  $\sim 90$ , 40, and 10 for wavelengths of 120, 140, and 160 nm, respectively.

#### 4.3. Photoelectric Yields of Olivine Grains

The olivine dust grains employed for the photoelectric efficiency measurements reported here were synthesized in the materials laboratory at the University of Alabama at Birmingham. These particles are of highly nonspherical configuration and were measured to be of effective radii in the range of 0.09–1.6  $\mu\text{m}$ . Figures 10a and 10b exhibit two examples of the measurements of photoelectric efficiency as a function of the surface potential,

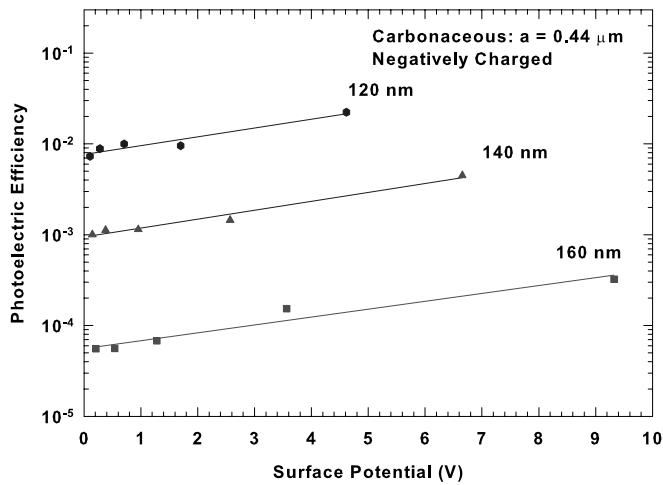


FIG. 8a

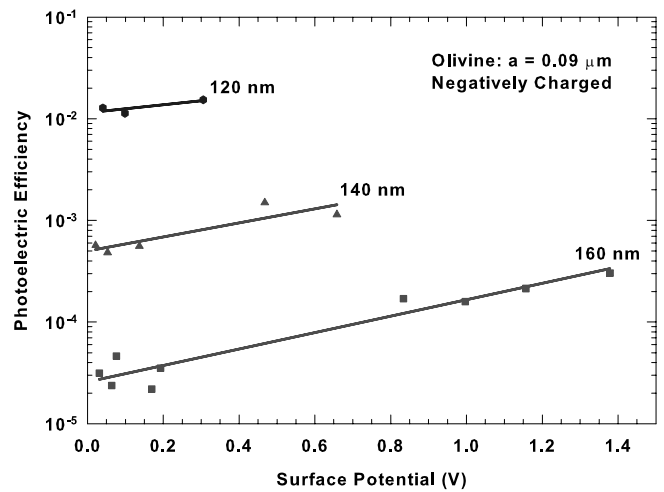


FIG. 10a

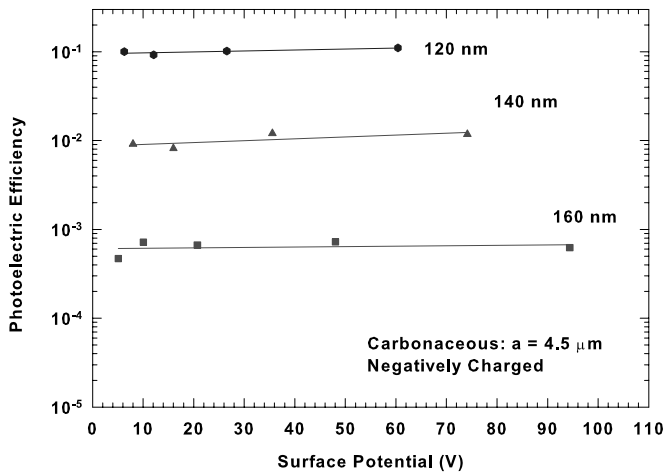


FIG. 8b

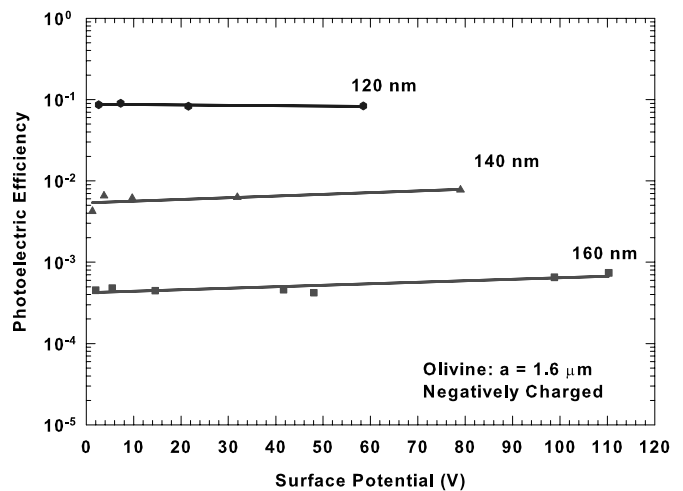


FIG. 10b

FIG. 8.—(a)–(b) Same as Fig. 4, but for two individual carbonaceous particles of 0.44 and 4.5  $\mu\text{m}$  radii. [See the electronic edition of the Journal for a color version of this figure.]

FIG. 10.—(a)–(b) Same as Fig. 4, but for two individual olivine grains of 0.09 and 1.6  $\mu\text{m}$  radii. [See the electronic edition of the Journal for a color version of this figure.]

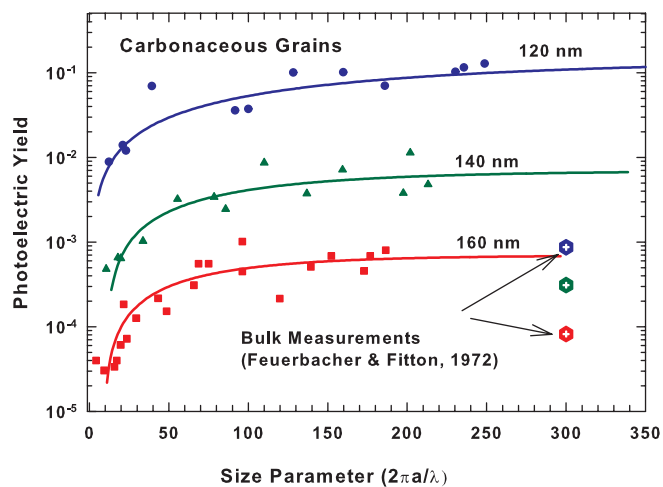


FIG. 9.—Photoelectric yield measurements on all carbonaceous particles as a function of the size parameter. Also shown are the measurements by Feuerbacher & Fitton (1972) made on bulk carbonaceous material for three photon energies of 10.3, 8.9, and 7.8 eV (120, 140, and 160 nm, respectively).

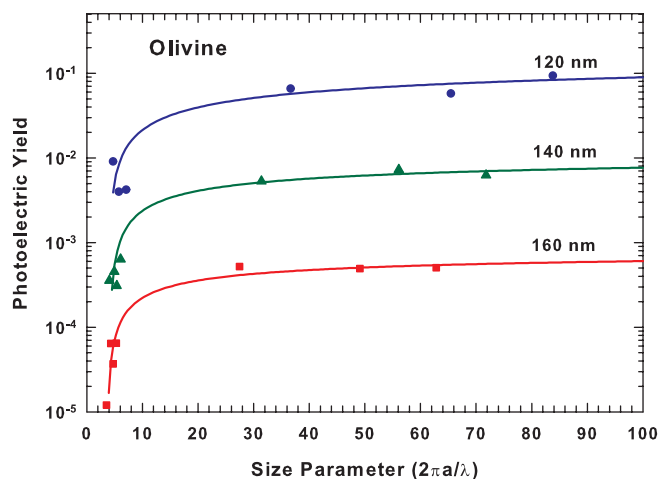


FIG. 11.—Photoelectric yields of all olivine particles of radii in the 0.09–1.6  $\mu\text{m}$  range as a function of the size parameter representing measurements at UV photon energies of 10.3, 8.9, and 7.8 eV (120, 140, and 160 nm, respectively).

conducted on two individual particles of 0.09 and 1.6  $\mu\text{m}$  radii. As in the previous cases, the measurements indicate a general dependence on the surface potential, in particular, for the smaller 0.09  $\mu\text{m}$  particle. A composite plot of the photoelectric yields as a function of the size parameter, representing measurements on eight particles of  $\sim 0.1$ –1.6  $\mu\text{m}$  radii is shown in Figure 11 at UV photon energies of 10.3, 8.9, and 7.8 eV (120, 140, and 160 nm, respectively). A general trend of higher yields for large size particles at all three wavelengths is indicated by the olivine particles, consistent with the silica and carbonaceous particles. To our knowledge, no photoelectric yield measurements on bulk materials for this material are available for comparison.

## 5. AN EXAMINATION OF POSSIBLE SOURCES OF ERRORS IN MEASUREMENTS

In view of the novel nature of the results presented in paper, we examine the potential sources of errors that may render the experimental values unreliable. In particular, sources of experimental errors that may lead to systematic effects relevant to the particle size are considered. As discussed in §§ 2 and 3 the measurement procedure and the analytical technique for determination of photoelectric efficiencies and yields are based on direct measurements of the quantities  $i_{\text{PMT}}(\lambda)$ , the UV beam width  $w_e(\lambda)$ , the effective diameter  $D_{\mu\text{m}}$  of the grain, and the charge as a function of time. The number of photons incident per second on the dust grain  $n_d^{\text{ph}}$  is determined by using equation (8). Also, the number of electrons emitted per second by the grain  $n_d^e$  defined by equation (9) is evaluated by direct measurement of the charge  $q$  and the discharge rate  $(\partial q/\partial t)$ . The photoelectric efficiency and yield is finally based on measurement of the quantities  $n_d^{\text{ph}}$  and  $(\partial q/\partial t)$  as defined in equations (8)–(11).

### 5.1. Measurement of Photons Incident on a Grain, $n_d^{\text{ph}}$

Evaluation of this quantity requires direct measurements of the following:

1. *The total number of photons per second in the UV beam  $N_B^{\text{ph}}$* : It is determined by projecting the beam on a PMT and measuring  $i_{\text{PMT}}(\lambda)$ . This is a direct measurement and provides an accurate value of  $n_B^{\text{ph}}$  with no systematic effects relevant to the particle size.

2. *The UV beam width  $w_e(\lambda)$* : It is evaluated by using the optical modeling program ZEMAX, with the calculated values validated by direct measurements by using the knife-edge method in the trap under vacuum. The measured beam width is  $\sim 3.5$ –4.5 mm and has no systematic size-dependent effect.

The above two measurements are made at pressures of  $\sim 10^{-4}$  torr. The nearly constant measurements of  $i_{\text{PMT}}(\lambda)$  at each wavelength indicate the consistency of  $n_d^{\text{ph}}$  from one particle to another, ensuring that the calculation of the number of photons per second in the beam remains nearly the same. With small variations in the measured values being incorporated in the calculations, there is no possibility of systematic size effects.

3. *Determination of grain effective diameter  $D_{\mu\text{m}}$* : For measurements of the photoelectric efficiency and yield of silica grains, spherical particles of predetermined diameters of 0.2–6.8  $\mu\text{m}$ , prepared and calibrated by Bangs Laboratory, Indiana, were employed. For other nonspherical particles, the effective diameters were determined by using the spring-point method that is based on marginal stability conditions as a function of the atmospheric drag at pressures of  $\sim 1$ –10 torr. This methodology was developed by acquiring a database with measurements of viscous drag factor  $\xi$  as defined in equation (2), on calibrated micron-size spherical particles of silica and polystyrene of predetermined

size. The validity of the measured database was evaluated with diameter measurements of particles of predetermined size by the spring-point method. The validation procedure involved laboratory prepared polystyrene particles of known size, large-size particles with approximate diameters determined by imaging on a monitor with magnification optics, and small-size particles with the size range limited by one-electron detection. The spring-point technique employed for size determination in the measurements presented here was validated by employing “blind” tests and found to provide effective diameters with uncertainties of less than 10%.

It should be noted that a random uncertainty in knowledge of the effective diameters only contributes to the scatter in the measurements of photoelectric emissions caused by the irregular shape of the particles as well as uncertainties in the measurable quantities. Systematic uncertainties in effective diameters, on the other hand, only lead to systematic shifts in the photoelectric yields with respect to the size parameter. A systematic uncertainty in size determination does not lead to a size-dependent effect in the photoelectric yields. The effect of uncertainties in the size parameter is clearly much smaller than the size dependence of the yields indicated by the measurements.

### 5.2. Measurement of the Grain Charge $q$ and Discharge Rate $(\partial q/\partial t)$

This measurement is most crucial for accurate evaluation of the photoelectric yields and requires careful scrutiny. The results on photoelectric emissions presented in this paper were made on negatively charged particles with a high initial charge  $q = Ze$  and discharged with UV radiation in sequences at three wavelengths of 120, 140, and 160 nm. The particles are discharged to  $Z$  values approaching zero at which they are ejected from the trap. The DC voltage  $V_{\text{DC}}$  required to keep the particle at the trap center is recorded as a function of time (Fig. 3), and the discharge rate is calculated in accordance with equation (9). In the following, we examine the accuracy of the charge measurements in view of the following potential sources of errors.

1. *How accurate is evaluation of the discharge rate  $(\partial q/\partial t)$* ? The discharge rate is determined from measurements of the change in the particle charge with time as shown in Figure 3. The particle charge  $q$  may be determined accurately with high sensitivities, approaching the detection limit of a single electron emission at a time in sufficiently low charge regimes. The discharge rate is calculated with a computer program that permits a running average over a variable interval of time or alternatively over a number of data points, determined by the nature of the measured data. The accuracy of this measurement is basically determined by the accuracy of the measurements of  $V_{\text{DC}}$ .

2. *Could the vibrational motion of a trapped particle move it in and out of the UV beam with systematic effects for large and small particles?* The effective particle diameters are  $\sim 0.1$ –15  $\mu\text{m}$ , whereas the beamwidth is  $\sim 3500$ –4500  $\mu\text{m}$ . The UV beam is aligned with the horizontal axis through the trap center. With amplitude of the vibrational motions being limited to maximum lengths of a few microns, the particle remains near the beam center as validated by the projected image on the monitor.

3. *Could the discharge rate be influenced by collisional processes with the ambient gas?* This effect is completely negligible since with the UV radiation turned off at pressure levels of 760 to  $\sim 10^{-5}$  torr, a charged particle may be kept trapped for several days at a time without any measurable change in the charge. The ionization potential (IP) of major gases in the trap ( $\text{N}_2$ ,  $\text{O}_2$ ) is much higher than the UV photon energies. In addition, the mean

free path at pressures  $\sim 10^{-5}$  to  $10^{-4}$  torr is so large that any effect due to the presence of positive ions would be completely negligible. A typical example of the effect of UV radiation on the discharge of a particle with charge  $q$  is shown in Figure 3 as a function of time with the corresponding DC voltage  $V_{DC}$ .

4. *What are the effects of differences in particle shapes and surface features on photoelectric emissions?* In our analysis, the particles of irregular shape and known density, with measurements of charge-to-mass ratio, are characterized by effective diameters. The photoelectric emission process is determined mainly by the particle size, with random differences in shapes and surface features reflected by the scatter in the data. This is indeed what is observed.

5. *Are there any effects of electron emissions from the walls illuminated with UV radiation?* The entrance and exit apertures for the UV beams are  $\sim 6$  mm, while the beam size is  $\sim 3.5$ – $4.5$  mm. The effects of any electrons emitted from the walls with incident UV radiation and colliding with negatively charged dust grains are expected to be negligible under a repulsive force of the negatively charged particles. Nevertheless, for cases in which the UV beam width is wider than the exit aperture, using equations (8)–(11), we estimate the fractional change  $\Delta Y$  in the photoelectric yield due to electrons emitted from the walls as

$$\Delta Y = 3.9 \times 10^{-9} \frac{Y_W}{Y_d} \eta_{\text{stick}} S_A, \quad (12)$$

where  $Y_W$  and  $Y_d$  are the photoelectric yields for the trap walls and the dust materials, respectively;  $\eta_{\text{stick}}$  is the efficiency of the photoelectrons for sticking to the negatively charged dust grains; and  $S_A$  ( $\mu\text{m}^{-2}$ ) represents the surface area of the walls exposed to UV radiation. It should be noted that any particle size dependence of  $\Delta Y$  in equation (12) enters only through  $Y_d$ , and there is no direct dependence on the particle size. If the  $Y_d$  is not size dependent, the electron emission from the walls would not produce a size-dependent effect. If, on the other hand,  $Y_d$  is higher for submicron-size particles, as expected by the current theory, the fractional change due to emission from the walls would be smaller for small-size particles, an effect contrary to the measured trend. In any case, the numerical values for  $\Delta Y$  for the beam diameter larger than the aperture by, say, 2–4 mm,  $Y_w = Y_d$ , and sticking efficiency  $\sim 0.1$  for the negatively charged particles is indicated to be  $< 1\%$ . From equation (12), we find the effect of electron emission from the walls to be negligibly small, for any realistic values of beam diameters, sticking efficiencies, and the relative yields of the grain and wall materials.

6. *What are the effects of the electrical fields of the DC voltage  $V_{DC}$  and the AC voltage  $V_{AC}$  on the measured photoelectric emission rates?* The role of the DC potential ( $\sim 0.05$ – $36$  V) applied to the top and bottom electrodes is only to produce a vertical field to balance the gravitational force and keep the particle at the trap center. The AC potential applied to the ring electrode, however, produces a null field at the trap center, and the suspended particle is confined to a region of relatively small electric field at frequencies of  $\sim 100$ – $800$  Hz.

The external AC and DC fields would influence the photoelectric emission rates only if they modify the WF or the threshold energy required for ejection of an electron from the dust particle. Field emission phenomenon occurs at electric field strengths several orders of magnitude higher than the AC or DC fields involved in the experiments reported here, and consequently we find the field emission effect due to applied potentials to be completely negligible.

The above conclusion is validated by the data relating to a whole series of experiments on a large number of particles involving a wide range of values of  $V_{DC}$ ,  $V_{AC}$ , and  $f_{AC}$ , where the particles discharge only when the UV radiation is turned on, with no significant difference in the discharge rates for similar particles at different values of  $V_{AC}$ . Figures 12a–12c exhibit three plots of measurements of the photoelectric efficiency, the AC potential  $V_{AC}$  as a function of grain-surface potential  $\phi_s$ , carried out on three similar silica grains at UV wavelength of 160 nm: (a)  $a = 0.33$   $\mu\text{m}$ ,  $V_{AC} \sim 1000$ – $2000$  V,  $\phi_s = 0.1$ – $1.4$  V; (b)  $a = 0.37$   $\mu\text{m}$ ,  $V_{AC} \sim 700$ – $2000$  V,  $\phi_s = 0.2$ – $1.8$  V; and (c)  $a = 0.38$   $\mu\text{m}$ ,  $V_{AC} \sim 250$ – $1000$  V,  $\phi_s = 1$ – $9$  V. The plots in the above figures indicate dependence of the photoelectric efficiency on grain surface potential or the charge as discussed previously. However, the efficiencies at similar surface potentials exhibit only small differences that are indicative of differences in the particle size and shape. The photoelectric yields corresponding to efficiencies for  $\phi_s \rightarrow 0$  indicate values of  $\sim (1.7$ – $2.6) \times 10^{-4}$  despite significant differences in the values of  $V_{AC}$ . Also, it is significant to note that the photoelectric efficiencies indicate a decreasing trend with increasing values of  $V_{AC}$ , which is opposite to what would be expected for enhanced emissions for higher AC potentials. We therefore conclude that the external fields have no influence on discharge rate of a trapped particle under UV illumination.

## 6. THEORETICAL MODELS AND COMPARISON WITH EXPERIMENTS

### 6.1. Theoretical Models on Size Dependence of Photoelectric Yields

In this section, we examine laboratory measurements of the photoelectric yields presented in this paper in view of the existing theoretical models and predicted values for micron/submicron-size dust grains. Detailed descriptions of the basic theory of photoelectric emissions are given in standard texts on solid-state physics (e.g., Cusack 1958; Kittel 1996). The electrons at the surface regions of neutral dust grains are considered to be confined to a potential well produced by a double layer of equal and opposite charges formed at the boundary of the grain and the surrounding medium. The double layer of atomic dimensions is assumed to be of order a few angstroms. The absorption of a UV photon in a dust grain leads to an excited electron moving toward the surface. The excited photoelectron may be ejected from the grain provided its energy is sufficiently high to overcome the energy lost in the inelastic scattering, penetrate or tunnel through the barrier formed by the double layer at the surface, and in addition is enough to overcome the attractive force due to the image potential of the ejected electron. With a positively charged grain of charge  $Ze$  ( $Z > 0$ ), an ejected electron experiences a strong attractive force at short distances, e.g., a few hundred angstroms from the surface due to the image potential, and is subjected to a long-range attractive Coulomb force at longer distances. With a negatively charged grain ( $Z < 0$ ), the ejected electron also experiences an attractive force at short distances from the grain ( $\sim 10$ – $500$  Å), due to the image potential, but is subjected to a repulsive Coulomb force at larger distances. A neutral insulating grain has all valence band energy levels occupied, and the excess electrons occupy the first available vacant energy levels in the conduction band, with the difference in the energy levels referred to as the “band gap.” Consequently, the energy required for ejection of an excess electron from the conduction band, also referred to as photodetachment, is less than that required for ejection of an electron from the valence band.

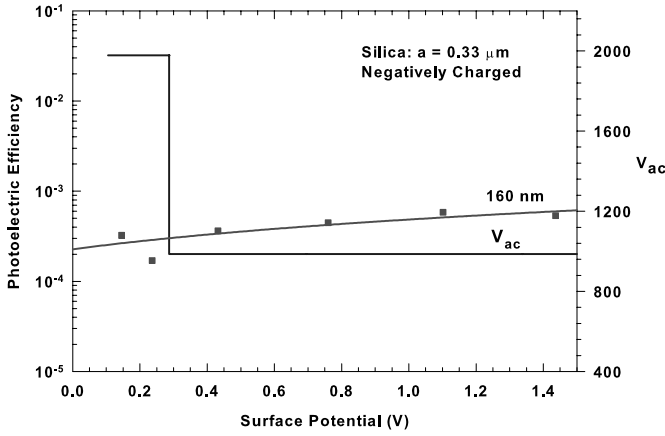


FIG. 12a

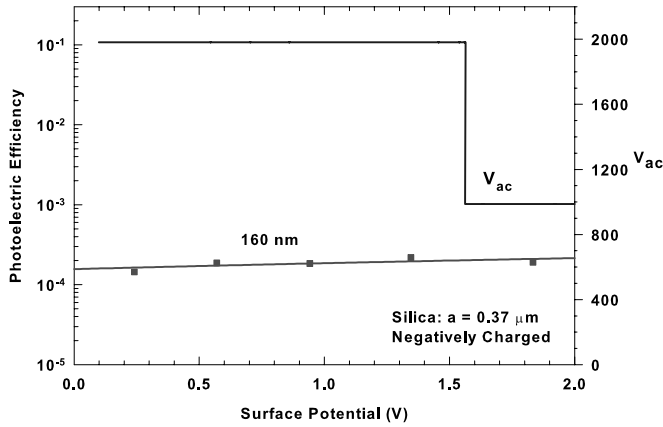


FIG. 12b

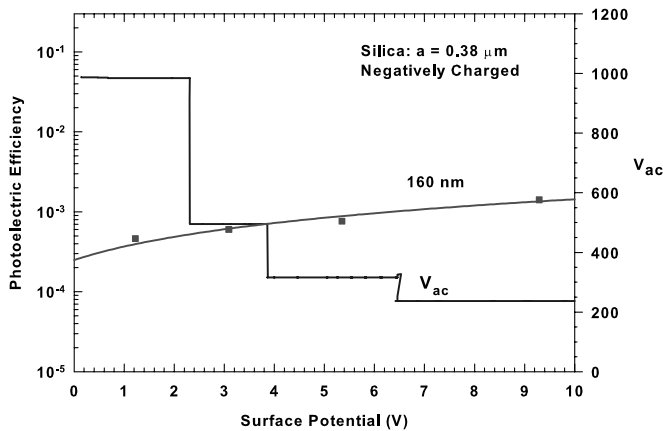


FIG. 12c

FIG. 12.—(a) Photoelectric efficiency of a negatively charged  $0.33 \mu\text{m}$  radius particle discharged with UV radiation at  $160 \text{ nm}$  wavelength from an initial surface potential of  $\sim 1.4\text{--}0.1 \text{ V}$ , at AC ring electrode peak potentials of  $\sim 1000$  and  $\sim 2000 \text{ V}$ . (b) Same as in (a), but for a particle of  $0.37 \mu\text{m}$  radius at AC ring electrode peak potentials of  $\sim 1000$  and  $\sim 2000 \text{ V}$  varied at different particle surface potentials of  $\sim 1.8\text{--}0.2 \text{ V}$ . (c) Same as in (a), but for a particle of  $0.38 \mu\text{m}$  radius at AC ring electrode peak potentials of  $\sim 250\text{--}1000 \text{ V}$  varied at different particle surface potentials of  $\sim 9\text{--}1 \text{ V}$ . [See the electronic edition of the *Journal* for a color version of this figure.]

No rigorous theoretical models of the photoelectric yields of individual small dust grains are available as yet. In the following we examine the predictions of the current theoretical models on size dependence of the WF, IPs, or ionization energies, and experimental validations of the models by measurements of the photoelectric yields.

1. According to a model adopted by Watson (1972), the probability of an electron being emitted from a solid after photon absorption at a distance  $x$  below the surface is proportional to  $\exp(-x/l_e)$ , where  $l_e$  is the electron escape length. The electrons that are excited deep inside the solid at distances larger than the attenuation length  $l_a$ , corresponding to an  $e$ -folding length of the radiation, do not reach the surface. The yield of small grains is assumed to be enhanced relative to the bulk values as the distance  $x$  of electron excitation to the surface is limited for small grains. Several reviews of theoretical evaluations of the photoelectric emissions have been given in the literature, in particular, on expected enhancements of the photoelectric yields of small dust grains in comparison with measurements for the corresponding bulk materials (e.g., Watson 1972, 1973; Draine 1978, 2004; Bakes & Tielens 1994; Weingartner & Draine 2001). Based on this consideration, Draine (1978) developed an expression for the yield enhancement factor for small grains of radii  $a$ , given by

$$y_1 = \left(\frac{\beta}{\alpha}\right)^2 \frac{\alpha^2 - 2\alpha + 2 - 2 \exp(-\alpha)}{\beta^2 - 2\beta + 2 - 2 \exp(-\beta)}, \quad (13)$$

where  $\alpha = a/l_a + a/l_e$  and  $\beta = a/l_e$ . The typical values for the two lengths  $l_e$  and  $l_a$ , from experimental data, are estimated to be  $\sim 10$  and  $100 \text{ \AA}$ , respectively, although the value for  $l_e$  is uncertain (e.g., Bakes & Tielens 1994; Hino et al. 1976; Pope & Swenberg 1982). For particle sizes corresponding to polycyclic aromatic hydrocarbon molecules, Bakes & Tielens (1994) estimated the yield enhancement to be  $\sim 11$  with the above choice of parameters. However, for particle sizes in the range of  $0.09\text{--}5 \mu\text{m}$  radii employed in the experiments reported here with the parameters discussed above, equation (13) does not predict any enhancement and the factor  $y_1$  approaches unity. This model predicts a constant value of the photoelectric yields with no variation over the size range considered, whereas the measurements indicate a size dependence with a sharp decrease in the yields for smaller sizes. The model described by equation (13) is thus not in agreement with the measurements made on individual dust grains presented in this paper.

2. Weingartner & Draine (2001) provided estimates of the threshold energy  $h\nu_{\text{pet}}$  for the photoelectric ejection of electrons from the valence band, as a function of grain charge and size. Here we reproduce their results but ignore quantum effects that are unimportant for the grains in our trap. For  $Z \geq -1$ ,

$$h\nu_{\text{pet}} = W_b + \left(Z + \frac{1}{2}\right) \frac{e^2}{a}. \quad (14)$$

Van Hoof et al. (2004) slightly modified the Weingartner & Draine result for  $Z < -1$ , finding

$$h\nu_{\text{pet}} = W_b - \frac{e^2}{2a} + (Z + 1) \frac{e^2}{a} \left[ 1 - \frac{1}{1 + (-Z - 1)^{-1/2}} \right]. \quad (15)$$

From equation (15), the threshold energy decreases as the grain becomes more negatively charged. This is in qualitative agreement with our result that the photoemission efficiency increases

with  $-Z$ . However, the shift in threshold energy is at most  $\sim 0.1$  eV for the grains considered here. From equation (14), the threshold energy for neutral grains decreases with size  $a$ . If this shift in threshold energy were the only factor influencing the yield, then the yield would increase with grain size. Weingartner & Draine (2001) also included the Watson size-dependent yield enhancement, so their model yields tend to increase as the grain size decreases (for  $a \lesssim 300$  Å). For the grains considered here, both the threshold energy shift and the Watson effect are expected to be negligible. Thus, this model is not in agreement with the measurements presented in this paper.

Parallel to the above developments of photoelectric yields of dust grains for astrophysical applications, a large body of literature exists on development of theoretical models for size dependence of the WFs, IPs, or the ionization energies of individual atoms, aggregates, or clusters of atoms (e.g., Gallo & Lama 1974, 1976a, 1976b; Ekaradt 1985; Seidl et al. 1991; Bréchnignac et al. 1992; Dugourd et al. 1992; de Heer 1993; Wong et al. 2003). The basic assumption in the development of these models is the expectation of evolution of the physical properties of small atomic systems progressing to large clusters and particles of arbitrary size. The models are designed to predict the energy required to remove an electron from an atomic system, with a systematic transition of the IP for single atoms to clusters of a few to a large number of atoms, and extending to the WF for bulk materials. In these models, the effective radii  $R_{cl}$  of a cluster of  $N$  atoms is assumed to vary as  $R_{cl} \propto N^{1/3}$ , with the predicted IP dependence on  $N$  varying as  $\propto N^{-1/3}$ . With the new techniques for production and experiments on atomic clusters, the models are being tested and validated for clusters of sizes ranging from a few to thousands of atoms (e.g., Ekaradt 1985; Seidl et al. 1991; Bréchnignac et al. 1992; Dugourd et al. 1992; de Heer 1993; Wong et al. 2003). The measurements exhibit a clear trend of lower IPs and therefore higher expected photoelectric yields for larger clusters. A brief summary of the theoretical ideas relevant to the measurements presented here is given in the following.

3. A classical electrostatic model for evaluation of the WF and ionization energy of an insulating sphere of arbitrary radius  $a$  and dielectric constant  $K$  was given by Gallo & Lama (1974, 1976a, 1976b). This formulation for estimation of the ionization energy, defined as the energy required to remove an electron from a sphere of arbitrary radius  $a$  to a distance  $r_0 = a + x_0$ , just outside the surface where all the kinetic energy is dissipated against short-range forces. The ejected electron has to overcome the electrostatic forces due to the residual positive charge on the sphere, the polarization of the sphere induced by the residual charge, and by the electron itself. The energy required to move an electron from  $r_0$  to infinity is derived as

$$\varepsilon = \int_{r_0}^{\infty} \mathbf{F} \cdot d\mathbf{r} = \left( \frac{e^2}{r_0 - a} \right) - e^2(K - 1) \sum_{n=0}^{\infty} \frac{n}{1 + n(K + 1)} \frac{a^n}{r_0^{n+1}} + \frac{1}{2} e^2(K - 1) \sum_{n=0}^{\infty} \frac{n}{1 + n(K + 1)} \frac{a^{2n+1}}{r_0^{2n+2}}. \quad (16)$$

The complex expression in equation (16) is approximated by

$$\varepsilon \cong \frac{e^2}{x_0} \left\{ 1 - \left( \frac{K - 1}{K + 1} \right) \left( \frac{a}{a + x_0} \right) + \left( \frac{1}{2} \right) \left( \frac{K - 1}{K + 1} \right) \left[ \frac{a^3}{(2a + x_0)(a + x_0)^2} \right] \right\}. \quad (17)$$

In the limit of very large particle radii, equation (17) reduces to

$$\varepsilon \equiv W = \left( \frac{e^2}{4x_0} \right) \left( \frac{K + 7}{K + 1} \right). \quad (18)$$

Plots of equations (17) and (18), shown in Figure 1 of Gallo & Lama (1976b), for insulated spherical particles as a function of radius  $a$  and dielectric constant  $K$  indicate that the ionization energy or the WF monotonically decreases with radius and approaches asymptotic values for large radii representing bulk materials. Also, the plots indicate the WFs for a particle of radius  $a$  decreasing with increasing values of the dielectric constant  $K$ . The size dependence indicated by these plots implies the photoelectric emissions and yields increasing with particle radii with the asymptotic values approaching the bulk measurements and higher yields for particles with materials of higher dielectric constant.

The size dependence of the yield measurements presented in this paper, which indicates an order of magnitude higher yields for the larger particles compared with the small submicron size, is thus qualitatively consistent with the trend of the above classical electrostatic model. It is interesting to note that the trend of dielectric constant dependence indicated by the yield measurements presented in this paper is also qualitatively consistent with the above model. The measurements for carbonaceous particles (Fig. 9) with dielectric constant of  $\sim 12$ – $15$ , compared with silica (Fig. 7) with dielectric constant of  $\sim 2.5$ – $3.5$ , are measured to be higher by a factor of 2–3 as expected from the model. Clearly, the above classical model is only an approximate representation, and a rigorous theoretical model remains to be developed.

4. A model developed by Wong et al. (2003) is based on classical electrostatics for studies of the size dependence of the WFs and IPs. It provides a scaling relation based on the image charge method for calculation of the energies required for removal of an electron from particles over a size range of individual atoms, clusters or small particles, and bulk materials. As in item (3) discussed above, the interpolation formula is based on the energy required to remove an electron from a distance  $d$  above the surface to infinity and is written as (Jackson 1975)

$$\phi(R) = \frac{e^2}{4d} \left[ \frac{1 + 4(d/R) + 6(d/R)^2 + 2(d/R)^3}{(1 + d/2R)(1 + d/R)^2} \right] = W\eta\left(\frac{d}{R}\right), \quad (19)$$

where  $\eta(d/R)$  represents the scaling function for particles of radius  $R$ . In the limiting cases of  $R \rightarrow \infty$ , the scaling reduces to unity, and the IP approaches the bulk WF  $W = e^2/4d$ . On the other hand, for particle sizes approaching atomic dimensions,  $d/R$  is  $\sim 1$ ,  $\eta(1) = 2$ , and the expression  $\phi(R)$  provides the ratio of the atomic IP to the WF of bulk material by the well-known value of  $IP/W \sim 2$ . Equation (19) indicates a size dependence of the photoelectric yields, with higher values of the IP and lower photoelectric yields for particles of smaller radii, and is consistent with the measurements presented in this paper. However, the above scaling function for size dependence may be considered only on a qualitative basis in view of the simple classical electrostatic model on which it is based, and the IPs of small grains may not be estimated accurately.

The size dependence indicated by the scaling function in equation (19) has been generally verified by a large variety of

measurements on clusters of sizes varying from a few atoms to several thousand alkali metal atoms, to nanometer and micron-size particles. These measurements indicate the trend of progressively decreasing IPs or WFs, implying higher photoelectric yields for larger particles, from individual atoms to clusters and submicron/micron-size particles (e.g., Müller et al. 1988; Seidl et al. 1991; Dugourd et al. 1992; de Heer 1993; Wong et al. 2003). The following two examples are of particular interest for examining the size dependence of the photoelectric yields.

a) The measurements by Bréchnignac et al. (1992) for evaluation of ionization cross sections of sodium clusters composed of 170–900 atoms. These measurements indicate a dramatic increase in the photoionization cross sections or the yields of clusters irradiated with photon energies of  $\sim 3$ –6 eV, when the cluster size increases from the number of atoms  $n = 170, 500, \text{ to } 900$ , consistent with the photoelectric yield size-dependence measurements presented in this paper.

b) The measurements by Müller et al. (1988) on finite-size silver particles of 2.7, 3.8, and 5.7 nm radii, indicate photoelectric yields for the 5.7 nm particles about a factor of 2 larger than for the 2.7 nm particles, at all photon energies in the range of  $\sim 4.6$ –5.6 eV. These measurements are in agreement with the size dependence of the measurements reported in this paper.

The size dependence and the general trend of the experimental data on photoelectric yields presented in this paper are thus qualitatively consistent with the theoretical  $\sim 1/a$  functional dependence of the WF or IP indicated by items (3) and (4) above. The results are also consistent with a large body of experimental data that covers a wide range of particle sizes extending from clusters consisting of a few atoms, large number of atoms, extending to nanometer and micron-size particles. No measurements are available for micron-size particles discussed in this paper. It should be emphasized that the theoretical considerations discussed above are based on semiclassical electrostatic theory, and the expressions for IPs or WFs involve assumptions that provide approximate estimates and trends only. Only a general qualitative consistency of the experimental data with the theoretical considerations can thus be expected. Rigorous theoretical expressions based on quantum mechanical considerations involving complex physical processes in detail are not yet available and need to be developed. We do not currently have a viable explanation as to why the photoelectric emission increases with  $-Z$  and grain size  $a$  for the submicron grains. Clearly, further work on theoretical and experimental front on the photoelectric emissions from small micron/submicron-size particles needs to be carried out.

## 7. SUMMARY AND CONCLUSIONS

We have presented the first direct measurements of the photoelectric yields of individual dust grains of silica, graphite, and olivine composition with effective radii in the 0.1–5  $\mu\text{m}$  range. The measurements were made by levitating negatively charged dust grains in an electrodynamic balance and illuminating them with UV radiation at 120, 140, and 160 nm wavelengths (10.3, 8.9, and 7.8 eV photon energies, respectively). The photoelectric yields are determined by directly measuring the discharge rates of the dust grains along with the incident photon flux. The

principal results and the conclusions of measurements are the following:

1. Photoelectric emission measurements on individual silica, carbonaceous, and olivine dust grains of  $\sim 0.1$ –5  $\mu\text{m}$  radii exposed to UV radiation in the 120–160 nm wavelength range (10.3–7.8 eV) indicate a size dependence of the photoelectric yields, increasing with the size parameter ( $x = 2\pi a/\lambda$ ) reaching asymptotic values for particles of large size ( $x \sim 200$ –300) and an order of magnitude smaller for small-size particles ( $x \sim 1$ ). This dependence is indicated for the dust grains of all three compositions, consisting of silica, carbonaceous, and olivine types, and for the three photon energies. The measured yields over the 10.3–7.8 eV photon energies vary by about 2 orders of magnitude, similar to the variations on bulk materials (e.g., Feuerbacher & Fitton 1972).

2. The size dependence of the yields presented in this paper are found to be in qualitative agreement with the size dependence predicted by classical electrostatic models applicable over the range of atom clusters extending from single atoms, large clusters, nanometer/micron-size particles, to bulk materials, and are consistent with a large body of experimental data over this range. The experimental evidence suggests that the WF and the threshold energy required for photoelectric emission of an electron from a dust grain is a function of the grain size, and this dependence extends to larger sizes than indicated by the classical image theory equations.

3. The asymptotic values of yields for large size parameters are found to be much larger than the available measurements on bulk materials. For carbonaceous particles, the measured photoelectric yields are larger by a factor  $\sim 30$ –60 compared with the available bulk measurements (Feuerbacher & Fitton 1972). No bulk measurements for pure silica or olivine particles are available to our knowledge.

4. The photoelectric efficiency, defined as electrons emitted per incident photon, is a function of the particle charge or surface potential. This functional dependence is observed to be stronger for small grains as compared with grains of large size. A viable theoretical explanation for this observation remains to be developed.

5. The experimental results presented here have important implications for the charge state of dust grains and the physical and dynamical processes in astrophysical and space environments, and are of particularly high interest in addressing the issues of dust in the lunar and Martian environments.

This work was supported by the Science Directorate at NASA Marshall Space Flight Center. We are grateful to Frank Six and John Davis for their encouragement and support during the course of this work, to Ann Whitaker and Ron Koczor for support and funding under the IRAD program, and to C. Ryland, J. Redmon, V. Coffey, and N. Martinez and for their assistance in the laboratory setup and maintenance. We are grateful to C. F. Gallo for bringing some important references to our attention and for some very useful discussions and comments, to Vitaly Kresin for a careful review of the manuscript and for very useful comments and suggestions, and to M. Harwit for helpful and encouraging comments. The work at the University of Alabama, Birmingham, was supported in part by NASA-EPSCoR (grant NCCS-580).

## REFERENCES

- Abbas, M. M., Craven, P. D., Spann, J. F., West, E., Pratico, J., Tankosic, D., & Venturini, C. C. 2002a, *Phys. Scr.*, T98, 99  
 Abbas, M. M., et al. 2002b, in *Proc. Laboratory Astrophysics Workshop*, ed. F. Salama (NASA CP-2002-21186; Washington: NASA), 180  
 Abbas, M. M., et al. 2003, *J. Geophys. Res.* 108, SSH2-1  
 ———. 2004, *ApJ*, 614, 781  
 Bailey, M. E., & Williams, D. A., eds. 1988, *Dust in the Universe* (Cambridge: Cambridge Univ. Press)

- Bakes, E. L. O., & Tielens, A. G. G. M. 1994, *ApJ*, 427, 822
- Bohren, C. F., & Huffman, D. R. 1983, *Absorption and Scattering of Light by Small Particles* (New York: Wiley)
- Bréchnignac, C., Cahuzac, Ph., Carlier, F., de Frutos, M., Leygnier, J., Roux, J. Ph., & Sarfati, A. 1992, *J. Phys. II*, 2, 971
- Burtscher, H., & Schmidt-Ott, A. 1982, *Phys. Rev. Lett.*, 48, 1734
- Burtscher, H., Schmidt-Ott, A., & Siegmann, H. 1984, *Z. Phys. B*, 56, 197
- Cusack, N. 1958, *The Electrical and Magnetic Properties of Solids* (London: Longmans)
- Davis, E. J. 1985, *Langmuir*, 1, 379
- de Heer, W. A. 1993, *Rev. Mod. Phys.*, 65, 611
- Draine, B. T. 1978, *ApJS*, 36, 595
- . 2004, in *The Cold Universe*, ed. A. W. Blain et al. (Berlin: Springer), 213
- Draine, B. T., & Lee, H. M. 1984, *ApJ*, 285, 89
- Draine, B. T., & Sutin, B. 1987, *ApJ*, 320, 803
- Dugourd, Ph., Rayane, D., Labastie, P., Vezin, B., Chevaleyre, J., & Broyer, M. 1992, *Chem. Phys. Lett.*, 197, 433
- Dwek, E., & Smith, R. K. 1996, *ApJ*, 459, 686
- Ekardt, W. 1985, *Phys. Rev. B*, 31, 6360
- Field, G. B., & Cameron, A. G. W., eds. 1975, *The Dusty Universe* (New York: Neale Watson)
- Feuerbacher, B., Anderegg, M., Fitton, B., Laude, L. D., Willis, R. F., & Grand, R. J. L. 1972, *Geochim. Cosmochim. Acta Suppl.*, 3, 2655
- Feuerbacher, B., & Fitton, B. 1972, *J. Appl. Phys.*, 43, 1563
- Feuerbacher, B., Willis, R. F., & Fitton, B. 1973, *ApJ*, 181, 101
- Gallo, C. F., & Lama, W. L. 1974, *IEEE Trans. Indust. Applications*, 1A-10, 496
- . 1976a, *IEEE Trans. Indust. Applications*, 1A-12, 7
- . 1976b, *J. Electrostatics*, 2, 145
- Harwit, M. 1998, *Astrophysical Concepts* (New York: Wiley)
- Hino, S., Sato, N., & Inokuchi, H. 1976, *Chem. Phys. Lett.*, 37, 494
- Horanyi, M., Robertson, S., & Walch, B. 1995, *Geophys. Res. Lett.*, 22, 2079
- Horanyi, M., Walch, B., & Robertson, S. 1998a, *Lunar Planet. Sci. Conf.*, 29, 1527
- Horanyi, M., Walch, B., Robertson, S., & Alexander, D. 1998b, *J. Geophys. Res.*, 103, 8575
- Jackson, J. D. 1975, *Classical Electrodynamics* (New York: Wiley)
- Kittel, C. 1996, *Introduction to Solid State Physics* (7th ed.; New York: Wiley)
- Mukai, T. 1981, *A&A*, 99, 1
- Müller, U., Schmidt-Ott, A., & Burtscher, H. 1988, *Z. Phys. B*, 73, 103
- Pelizzari, M. A., & Criswell, D. R. 1978, *Lunar Planet. Sci. Conf.*, 9, 3225
- Pope, M., & Swenberg, O. E. 1982, *Electronic Processes in Organic Crystals* (Oxford: Clarendon)
- Schmidt-Ott, A., Shurtenbrger, P., & Siegmann, H. C. 1980, *Phys. Rev. Lett.*, 45, 1284
- Seidl, M., Meiwes-Broer, K.-H., & Brack, M. 1991, *J. Chem. Phys.*, 95, 1295
- Spann, J. F., Abbas, M. M., Venturini, C. C., & Comfort, R. H. 2001, *Phys. Scr.*, T89, 147
- Stubbs, T. J., Vondrak, R. R., & Farrell, W. M. 2006, *Adv. Space Res.*, in press
- van Hoof, P. A. M., Weingartner, J. C., Martin, P. G., Volk, K., & Ferland, G. J. 2004, *MNRAS*, 350, 1330
- Watson, W. D. 1972, *ApJ*, 176, 103
- . 1973, *J. Opt. Soc. Am.*, 63, 164
- Weingartner, J. C., & Draine, B. T. 2001, *ApJS*, 134, 263
- Wiscombe, W. J. 1979, *Mie Scattering Calculations: Advances in Technique and Fast, Vector-Speed Computer Codes*, *Nat. Cent. Atmos. Res. Tech. Note TN-140+STR* (Doc. PB301388; Springfield: NTIS)
- Wong, K., Vongehr, S., & Kresin, V. V. 2003, *Phys. Rev. B*, 67, 035406
- Wyatt, S. P. 1969, *Planet. Space. Sci.*, 17, 155